An Incremental Collapse Model for Metal Fatigue

Un modèle incrémental de rupture à la fatigue d'un métal

Ein inkrementales Bruchmodell zur Prüfung der Metallermüdung

S.A. GURALNICK
Professor of Civil Engineering
Illinois Institute of Technology, Chicago

Introduction

A number of attempts [1, 2, 3 and 4] have been made in the past to explain by means of mechanical models, or other analog systems the puzzling, and apparently even contradictory, set of phenomena which are comprised in metal fatigue. Previous attempts have been largely unsatisfactory because the models used were chosen in order to display a response which was analogous to a few gross macroscopic aspects of metal fatigue but could not be "stretched" to simulate the entire spectrum of observable phenomeny. These deficiencies may be largely overcome if the model (or analogue) chosen is the hyperstatic portal frame shown in Fig. 1. This structure has been treated by conventional analytical methods by NEAL [5] and experimentally by Neal and SYMONDS [6].

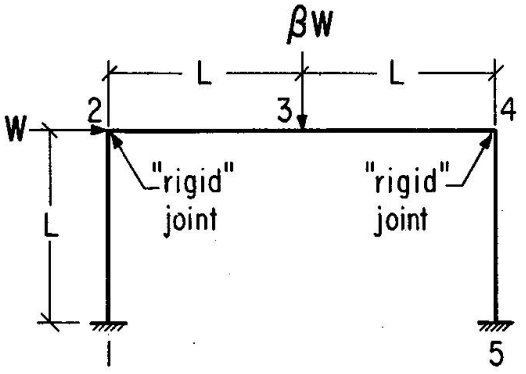

Fig. 1. Three-bar hyperstatic portal frame.

The Model

If the flexural members of the structure of Fig. 1 are uniform in cross section, are made of an elasto-plastic material whose stress-strain behavior is similar to that

diagrammed in Fig. 2a, they display the bending moment versus curvature response (linear-perfectly plastic) shown in Fig. 2b; and if the structure is subjected to repeated cycles of loading, the first sequence of which is shown in Fig. 3; then, for $\beta = 1$, the alternating plasticity load is,

$$W_a = 2.759 \frac{M_p}{L}; \tag{1}$$

the shakedown load is,

$$W_s = 2.857 \frac{M_p}{L}; \tag{2}$$

and, the plastic collapse load is,

$$W_c = 3 \frac{M_p}{L}. \tag{3}$$

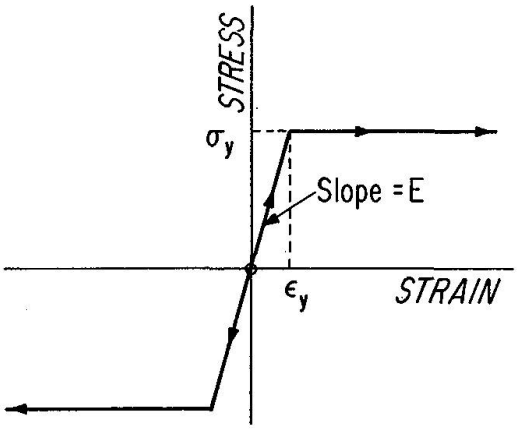

Fig. 2a. Stress Versus Strain.

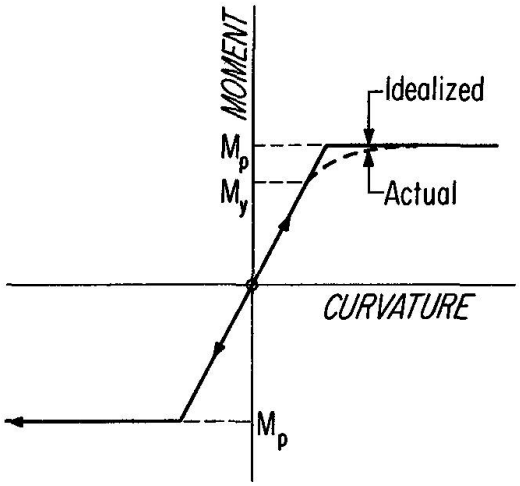

Fig. 2b. Bending moment versus curvature.

The mechanism of collapse corresponding to a monotonic increase in the loads to the collapse level is shown in Fig. 4. Additional values of W_a, W_s, and W_c are given in Table 1 for $\beta = 0.5$, 1, 1.5, and 2.

Table 1

Load	β	0.5	1.0	1.5	2.0
Alternating Plasticity	$\frac{W_a L}{M_p}$	2.750	2.425	2.049	1.665
Shakedown	$\frac{W_s L}{M_p}$	3.478	2.857	2.264	1.875
Plastic Collapse	$\frac{W_c L}{M_p}$	4.00	3.00	2.40	2.00

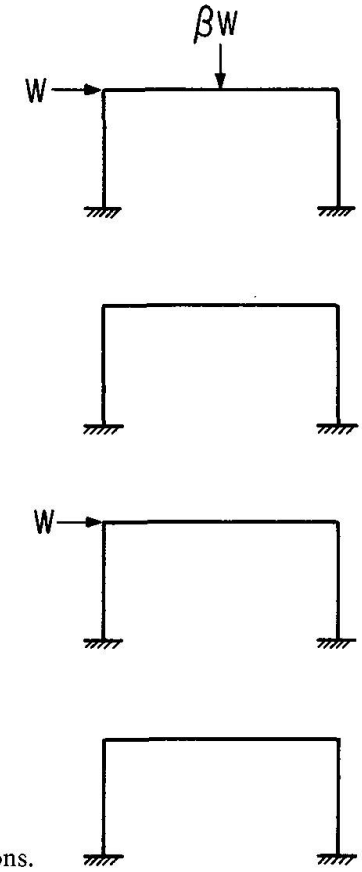

Fig. 3. One cycle of load applications.

If the more generalized cyclic load pattern of Fig. 5 is applied to the model and if the hysteresis energy ΔU generated in each cycle at various load ranges is computed, then the results may be displayed in graphs such as those shown in Fig. 6 for $\overline{W} = 0.5\ W_s$ and $\beta = 1.0$. Similar graphs may be obtained for all relevant values of $\overline{W}$ and β. An examination of all such graphs reveals that, depending on load range and mean load, one of two types of cyclic hysteresis may occur: If for a particular mean load $\overline{W}$ the load range R *lies* below a certain limiting value R^*, then the hysteresis energy ΔU decreases to zero as N increases. This form of hysteresis is sometimes called "elastic hysteresis". On the other hand, if for a particular mean load $\overline{W}$ the load range R exceeds the limiting value R^*, then the hysteresis is called "asymptotic hysteresis." GURALNICK [7] has shown that R^* is a continuous

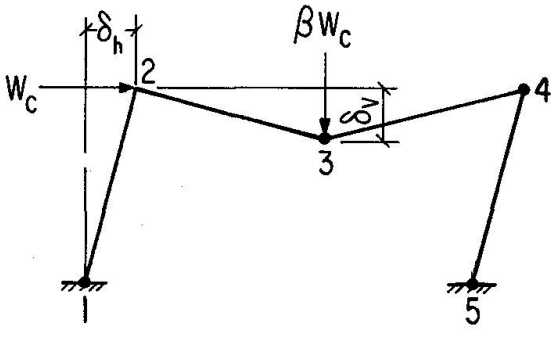

Fig. 4. Collapse mechanism.

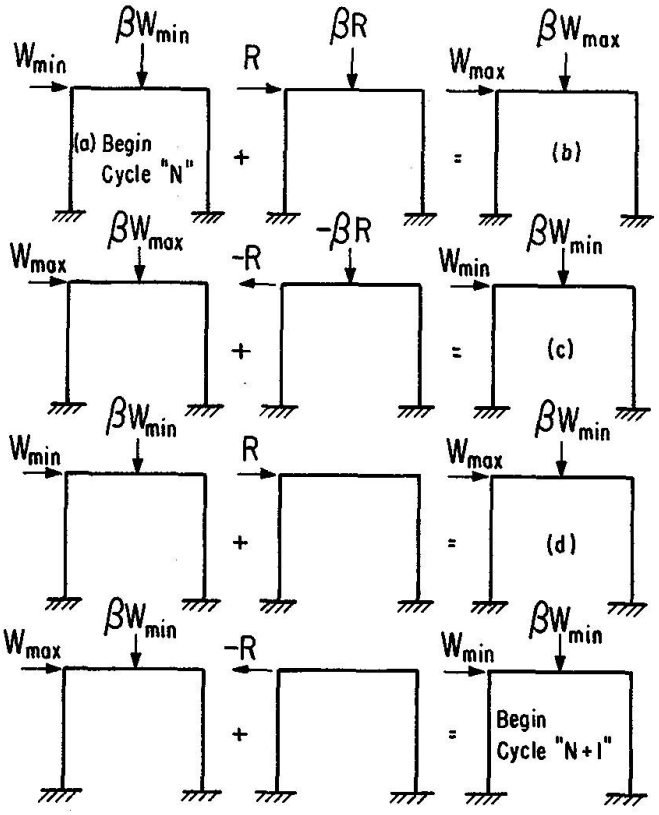

Fig. 5. The N^{th} cycle of load applications.

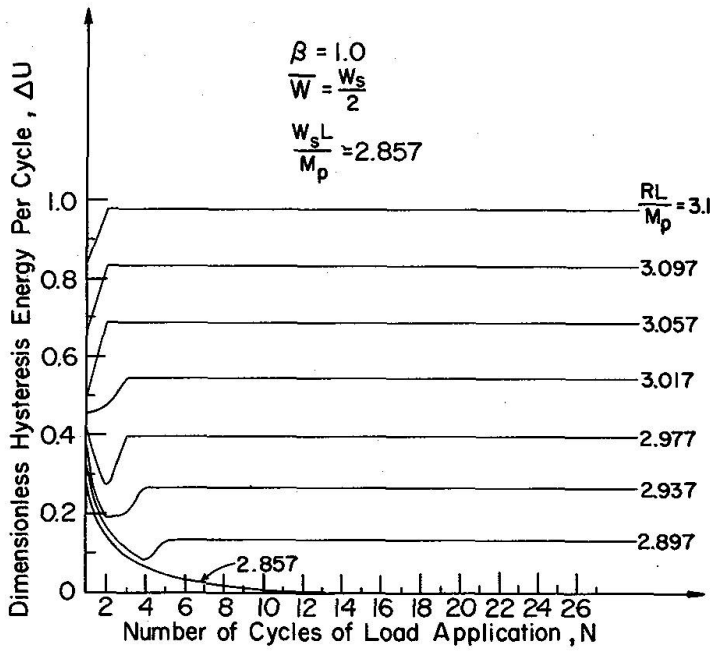

Fig. 6. Hysteresis energy per cycle versus number of cycles of load application.

function of the mean load $\overline{W}$. The results of a simple computerprogram which determines ΔU at the end of each cycle of load levels for prescribed mean loads may be used to construct graphs of the type displayed in Fig. 7. Because maximum and minimum loads are defined in terms of range R and mean load $\overline{W}$, the results displayed in Fig. 7 may be expressed as a family of envelopes, called "extended incremental collapse envelopes," as shown in Fig. 8 for various values of β in the range $0.5 < \beta < 2$. In Figs. 7 and 8 the curves corresponding to $\beta = 1$ have been emphasized for clarity. It may be observed from the $\beta = 1$ curve in Fig. 8, that values of W_a, W_s and W_c may be inferred which are in perfect agreement with the respective values given by Eqs. 1, 2, and 3 even though these latter three values were obtained by using conventional methods of "plastic analysis" rather than a computational process involving a consideration of hysteresis energy occurring during each cycle of load applications.

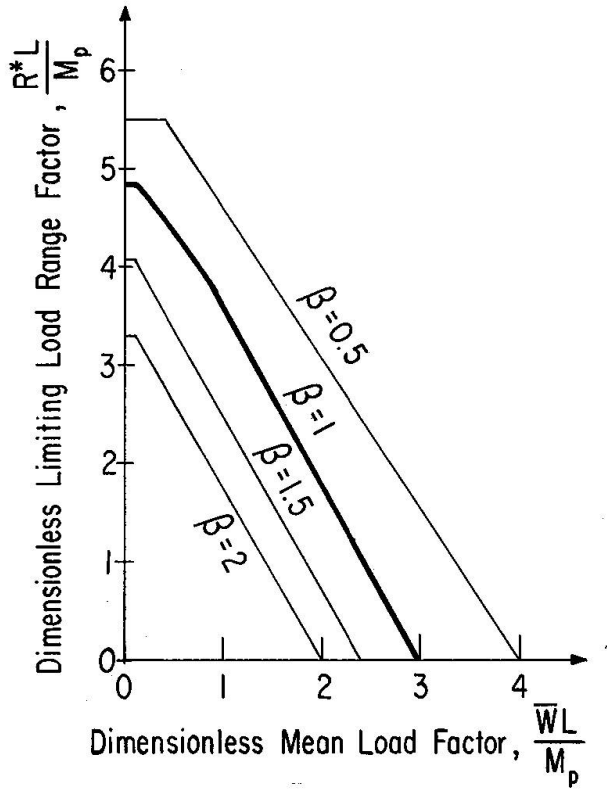

Fig. 7. Load range factor versus mean load factor diagrams.

If the initial direction of loading shown in Fig. 5 is reversed and if this reversed pattern of loading is applied to the model, then diagrams geometrically similar to those of Fig. 8 may be constructed except that algebraic signs will be reversed. If such diagrams for reversed loading are combined with those of Fig. 8 then the "complete" maximum or minimum load factor versus load factor diagrams of Fig. 9 will result. These diagrams, of course, are completely analogous to the conventional GOODMAN [9] — GERBER [8] diagram for metal fatigue. The diagrams of Fig. 9 are completely symmetrical whereas it is well known that such diagrams for real materials are unsymmetrical.

The graphs of cyclic hysteresis energy versus number of cycles of load application shown in Fig. 6 are particularly interesting because both strain softening and strain

hardening behavior is exhibited in the asymptotic hysteresis spectrum in addition to the aforementioned elastic hysteresis. Curiously enough, graphs similar to those of Fig. 6 for other values of $\overline{W}$ and β do not always display elastic hysteresis. Hence, it may be inferred that elastic hysteresis is a function of mean load as well as load range. This is indeed true as may be seen in Fig. 10 in which the loads producing the onset of elastic hysteresis are defined by the innermost set of lines which appear on the partial Goodman-Gerber type diagrams. This behavior of the model helps to clear up an aspect of the relationship between hysteresis and fatigue in materials that has puzzled many investigators ever since FÖPPL [10] noted that it is possible in some instances to observe hysteresis in a cyclic test even though the material does not fail in fatigue. This observation may now be clearly placed in its proper perspective by distinguishing between elastic hysteresis and asymptotic hysteresis. Furthermore, it is clear from the diagrams of Fig. 10 that elastic hysteresis may be present under some conditions (fluctuating or pulsating loads) and not appear in others (fully reversed alternating loads) even though the same material is being stress cycled.

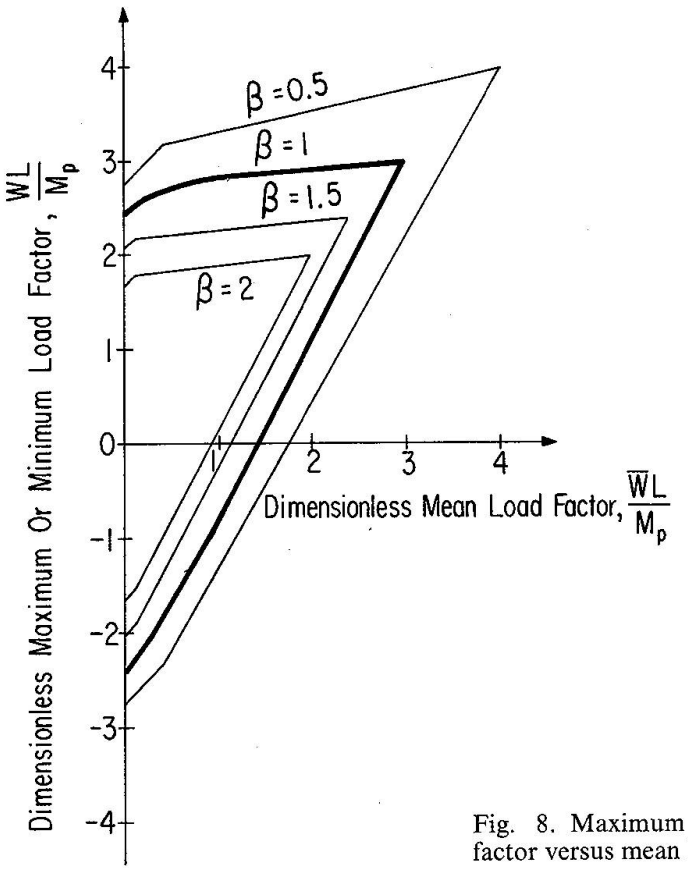

Fig. 8. Maximum or minimum load factor versus mean load factor diagrams.

The hysteresis energy dissipated in each cycle of load applications may be summed to obtain the cumulative hysteresis energy imparted to the structure at the end of the Nth cycle according to the relationship,

$$U = \sum_{i=1}^{N} \Delta U_i \tag{4}$$

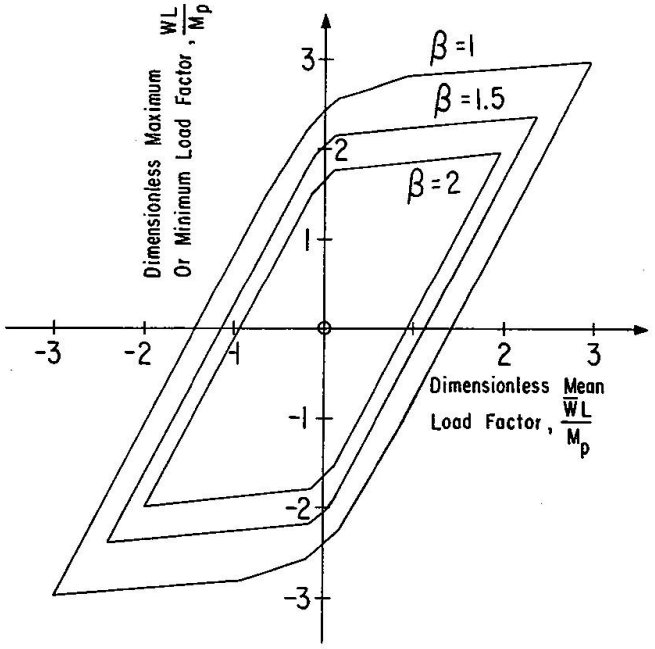

Fig. 9. Complete load factor versus mean load factor diagrams.

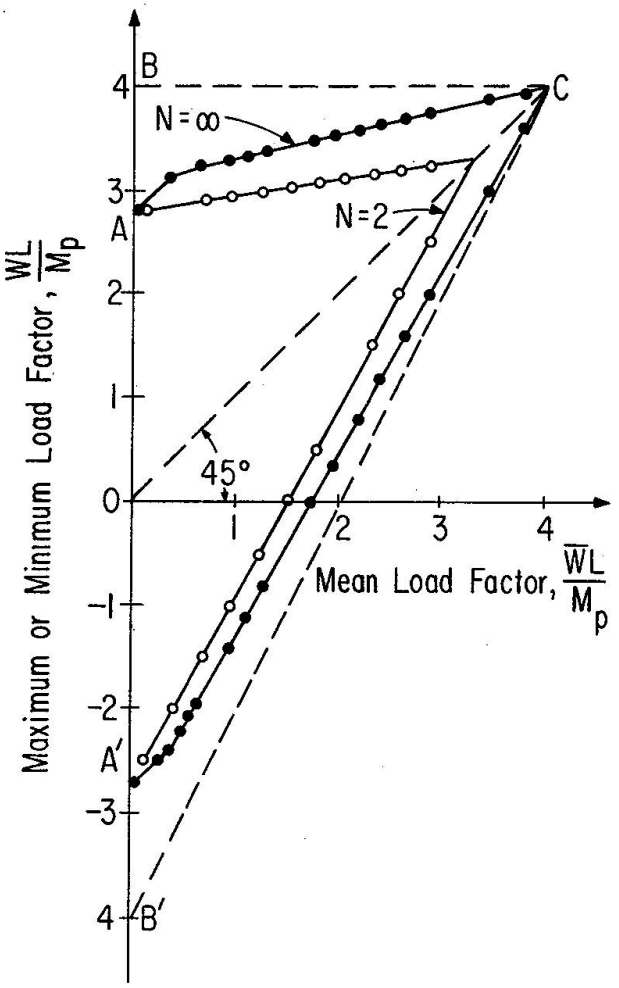

Fig. 10. Load factor versus mean load factor diagrams, $\beta = 0.5$.

in which ΔU_i is the hysteresis energy appearing in the ith cycle. A typical set of graphs of cululative hysteresis energy versus number of cycles of load application are shown in Fig. 11 for $\overline{W} = 0.5\ W_s$ and $\beta = 1.0$.

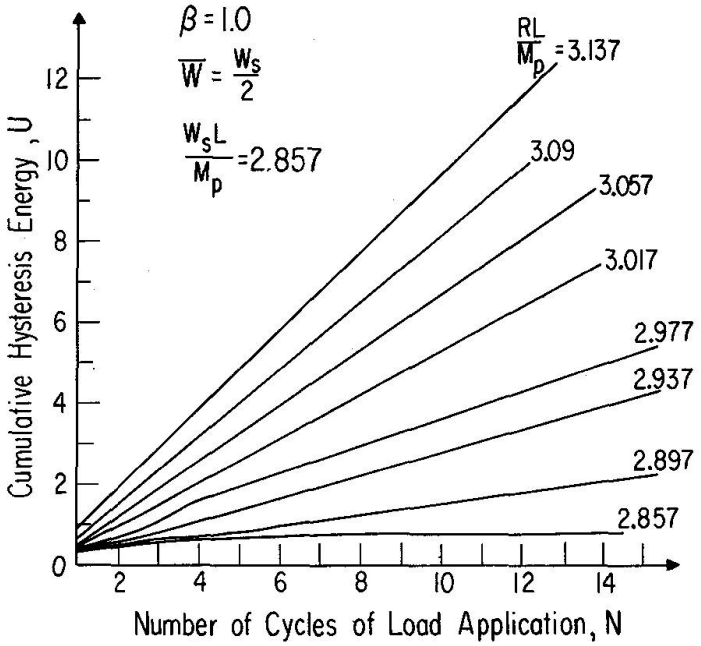

Fig. 11. Cumulative hysteresis energy versus number of cycles of load application.

The ability of any real structure to absorb hysteresis energy is finite and, hence, it may be argued that failure occurs when,

$$\sum_{i=1}^{N_F} \Delta U_i = U_F, \tag{5}$$

in which N_F is the extended incremental collapse life and U_F is the extended incremental collapse toughness. There is an obvious analogy between Eq. 5, representing the behavior of the model, and the behavior of metals in fatigue where U_F of the model is analogous to Ω_f, the "fatigue toughness" (c.f. HALFORD [11]).

Returning to the graphs of Fig. 10, it is known that if load range is confined to the region of the diagram bounded by the curves AC and $A'C$, then failure will not occur no matter how many cycles of load are applied to the model. If load range is allowed to exceed these boundary curves[1] and the loads penetrate into the regions ABC and $A'B'C$, then failure occurs when a finite number of load cycles have been applied.

Asymptotic hysteresis prevails in the regions ABC and $A'B'C$ in Fig. 10 and failure will occur, as argued above, when the cumulative hysteresis energy reaches the value U_F. Additional information may be derived if it is assumed that U_F is a linear function of the number of cycles to failure, or,

$$U_F = U_0 + MN, \tag{6}$$

[1] Of course, cyclic loads with a load range which exceeds the bounds defined by the lines BC and $B'C$ cannot be applied to the model because collapse in a single cycle would occur.

in which M is a constant. If the graph of Eq. 6 is plotted on the same diagram as a set of U versus N curves for a particular mean load and a particular value of β then a diagram such as that sketched in Fig. 12 results. Each curve of U versus N for a particular load range R_j may be approximated by a straight line of the form,

$$U = b_j + m_j N \tag{7}$$

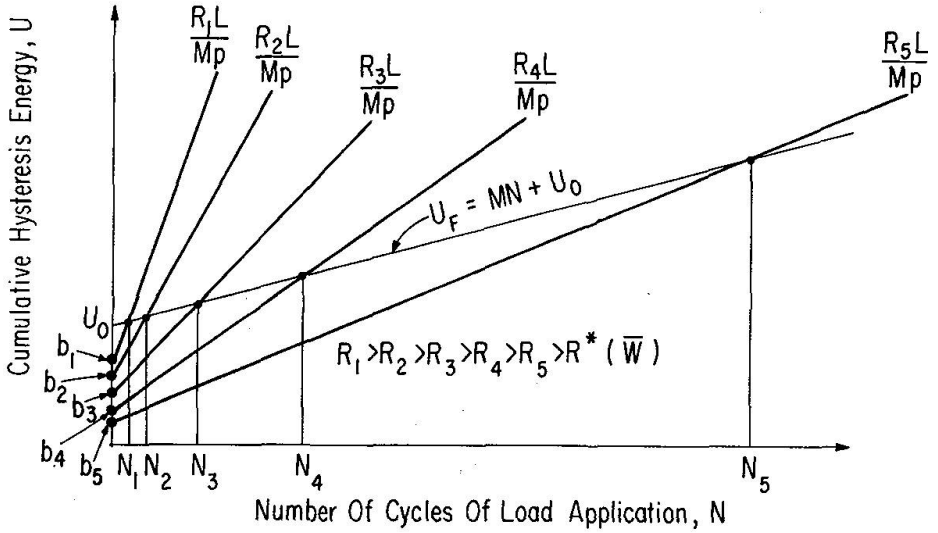

Fig. 12. Cumulative hysteresis energy versus number of cycles of load application.

in which b_j and m_j are constants defined for the corresponding load range R_j. For any particular load range R_j, the point of intersection of a line representing Eq. 7 with the line representing Eq. 6 has an N-coordinate on Fig. 12 which is the extended incremental collapse life N_{Fj}. The collection of R_j and N_{Fj} values for a particular value of mean load $\overline{W}$ and load ratio β is a set of ordered pairs and, hence, it may be argued that load range at failure and extended incremental collapse life are connected by a functional relationship which, for any particular set of values for $\overline{W}$ and β, may be written in the form,

$$\left.\frac{RL}{M_p}\right|_{\substack{\overline{W} \\ \beta}} = f(N_F). \tag{8}$$

Typical graphs of Eq. 8 for $\beta = 0.5$ and $\overline{W} = 0$ and $\overline{W} = 0.5\ W_s$ are shown in Fig. 13. The resemblance of the curves shown in Fig. 13 to conventional $S - N$ diagrams for the fatigue of ferrous metals is remarkable. In this regard, it may be observed that the limiting load range R^* (cf. Fig. 13) of the model is completely analogous to the endurance limit or fatigue limit displayed by cyclically stressed ferrous metals. Of course the graphs shown in Fig. 13 are merely contour lines projected on the load range versus life plane of the entire extended incremental collapse surface expressed in the coordinates of load range, mean load and life.

Such a surface for $\beta = 0.5$ is shown in Fig. 14. It is, of course, the analogue of the Fatigue Strength versus Mean Stress and Fatigue Life diagram proposed by STÜSSI [12].

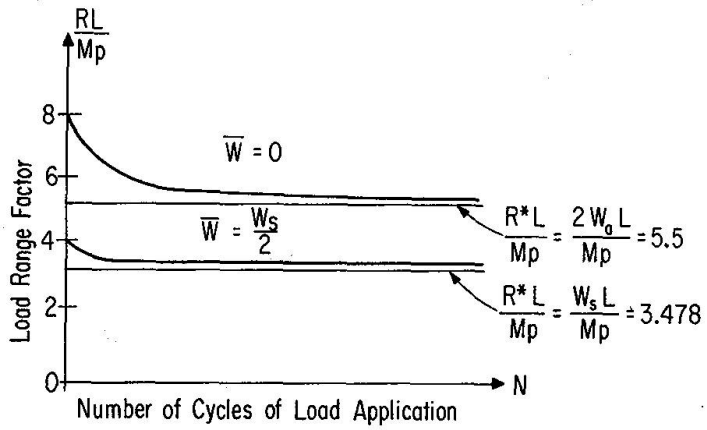

Fig. 13. Load range factor versus number of cycles of load application for $\beta = 0.5$.

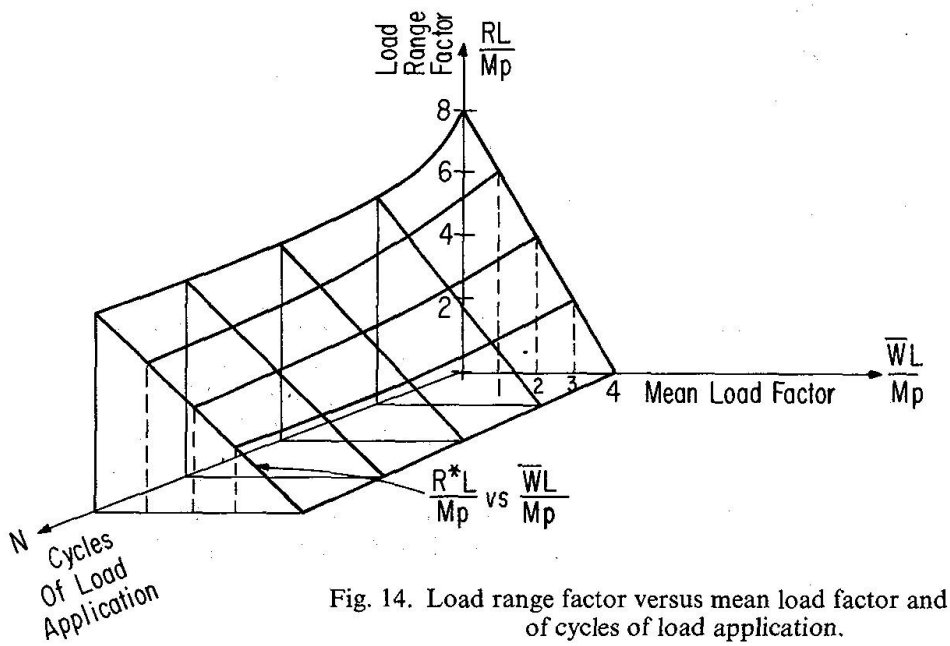

Fig. 14. Load range factor versus mean load factor and number of cycles of load application.

Among the several important observations made by HORNE [13] concerning the shakedown condition, he stated that,

(*i*) "The shakedown condition is unaffected by initial stresses however caused, so that these have no effect on whether or not a structure can shake down under a given set of loads. Initial stresses may, however, affect the number of load variations which have to take place before a condition of shakedown is actually reached."

and

(*ii*) "The order in which loads are applied has no effect on whether a structure can shake down, although again the order of loading may influence the rapidity with which a shakedown state is reached."

These two observations apply equally well to the entire extended incremental collapse envelope (cf. Fig. 9) instead of merely to one point on this envelope (i.e. the point defined by a cyclic load pattern with maximum load equal to the shakedown load W_s) and they may be restated as a principle.

Principle 1. The shape of the extended incremental collapse envelope for any particular value of β is neither affected by previous load history nor by the order in which loads are applied.

For all load patterns with a range which lies outside of the incremental collapse envelope, asymptotic hysteresis occurs. This means that, except for slight perturbations which occur during the first few cycles, the hysteresis energy per cycle rapidly approaches a constant value which depends only on load range, mean load and β and is independent of previous load history. These observations may also be stated as a principle.

Principle 2. If a cyclic pattern of loads is imposed on a structure such that the mean load and load range are constant and the load range lies outside of the corresponding incremental collapse envelope (or, load range $R > R^*$), then the hysteresis energy per cycle ΔU rapidly approaches a constant which depends only on load range, mean load and β and is independent of prior load history.

It may be inferred from Principles 1 and 2 that if the model is subjected to a sequence of load regimes each having a particular constant mean load and constant load range such that $R > R^*$, then the total hysteresis energy U is merely the sum of the hysteresis energies accumulated during each individual load regime and may be written as,

$$U = \sum_{i=1}^{n_1} \Delta U(R_1, \overline{W}_1)_i + \sum_{j=1}^{n_2} \Delta U(R_2, \overline{W}_2)_j + \sum_{k=1}^{n_3} \Delta U(R_3, \overline{W}_3)_k + \ldots \tag{9}$$

in which the typical term $\Delta U(R_p, \overline{W}_p)_q$ is the increment of hysteresis energy, for a particular set of values R_p and $\overline{W}_p$, accumulated during the 8th cycle of load applications. If the $\Delta U(R_p, \overline{W}_p)_q$ are independent of the number of cycles (i.e. independent of q) then Eq. 9 may be written as,

$$U = n_1 \Delta U(R_1, \overline{W}_1) + n_2 \Delta U(R_2, \overline{W}_2) + n_3 \Delta U(R_3, \overline{W}_3) + \ldots \tag{10}$$

Of course if the sequence of load applications is continued until failure by incremental collapse occurs, then U in Eq. 9 becomes U_F and,

$$n_1 + n_2 + n_3 + \ldots = N_F, \tag{11}$$

in which N_F is the extended incremental collapse life.

Fig. 11 clearly indicates that for any constant value $\overline{W}_p$ and R_p in excess of $R^*(\overline{W}_p)$, the graph of U versus N is, for all practical purposes, a straight line which may be written in the form,

$$U = m_i N + b_i, \tag{12}$$

as shown in Fig. 12. If the model is subjected to a sequence of load regimes each having a particular mean load $\overline{W}_p$ and load range R_p such that $R_p > R^*(\overline{W}_p)$, then according to Eq. 10 the total hysteresis energy U is merely the sum of the hysteresis energies accumulated during each individual load regime. This statement

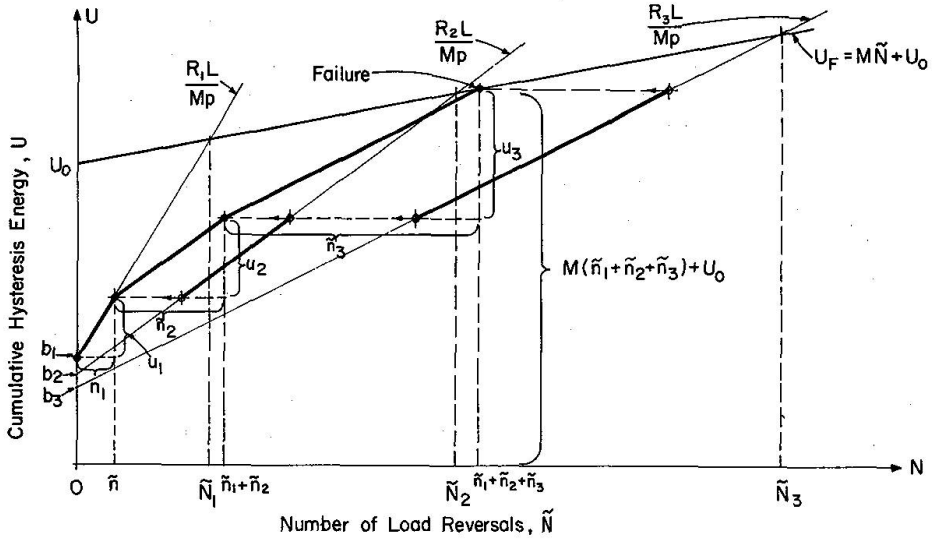

Fig. 15. Growth of hysteresis energy with number of load reversals.

may be represented by the three connected line segments starting at the point $(0, b_1)$ in Fig. 15. Failure occurs when the third line segment intersects the U_F – line[1]. Considering the geometry of the diagrams shown in Fig. 15, together with the equations of the lines, one may write,

$$\frac{\tilde{n}_1}{\tilde{N}_1}+\frac{\tilde{n}_2}{\tilde{N}_2}\left(\frac{U_0-b_2}{U_0-b_1}\right)+\frac{\tilde{n}_3}{\tilde{N}_3}\left(\frac{U_0-b_3}{U_0-b_1}\right)=1$$

or, in general, for a total of p load sequences,

$$\frac{\tilde{n}_1}{\tilde{N}_1}+\frac{\tilde{n}_2}{\tilde{N}_2}\left(\frac{U_0-b_2}{U_0-b_1}\right)+\ldots+\frac{\tilde{n}_p}{\tilde{N}_p}\left(\frac{U_0-b_p}{U_0-b_1}\right)=1 \tag{13}$$

in which the tilde mark denotes load reversals rather than load cycles. Since the number of load reversals is simply twice the number of load cycles, Eq. 13 may be rewritten as,

$$\frac{n_1}{N_{F1}}+\frac{n_2}{N_{F2}}\left(\frac{U_0-b_2}{U_0-b_1}\right)+\ldots+\frac{n_p}{N_{Fp}}\left(\frac{U_0-b_p}{U_0-b_1}\right)=1 \tag{14}$$

in which N_{Fp} is the fatigue life corresponding to a particular set of values $\overline{W}_p$ and R_p. If the quantities $b_1, b_2, \ldots, b_p$ are roughly equal to one another and/or they are very small compared to U_0, Eq. 14 reduces to the considerably simpler form:

$$\frac{n_1}{N_{F1}}+\frac{n_2}{N_{F2}}+\ldots+\frac{n_p}{N_{Fp}}=1. \tag{15}$$

It is clear that Eq. 15 is the exact analogue of the well-known "Cumulative Damage" or Palmgren-Miner Law for metal fatigue (cf. PALMGREN [14],

[1] The equation of this line is given by Eq. 6.

MINER [15], GROVER [16], KAECHELE [17] and LEVE [18]). Furthermore, insofar as the model is concerned, Eq. 15 is applicable regardless of the magnitude of $\overline{W}$ (provided that it is smaller than W_c) and regardless of the exact sequence of load applications (i.e. high loads followed by low loads or low loads followed by high loads). The only information one needs to have in order to use Eq. 15 for the model is the information contained in Fig. 14 and a specification of all but one of the values of $n_1, n_2, ..., n_p$. It is also worth noting that Eqs. 14 and 15 are apparently independent of the slope M of the U_F-line given by Eq. 6. Insofar as the derivation of these equations is concerned, there would be no difference in the result if it were assumed that $M = 0$. On the other hand, as was shown earlier, the values of $N_{F1}, N_{F2}, ..., N_{Fp}$ are clearly influenced by the character of the U_F versus N relationship.

Discussion and Conclusions

A consideration of the response of a simple portal frame model to cyclically applied loads reveals that localized plastic yielding alone is sufficient to cause behavior which simulates practically all of the gross macroscopic phenomena (in the purely deterministic sense) associated with metal fatigue. Hysteresis strain energy is widely recognized as an important macroscopic manifestation of the fatigue process in metals. The work of FELTNER [19], MARTIN [20], MORROW [21], CHANG [22] and LANDGRAF [23] is particularly noteworthy in this regard. It has been repeatedly (c.f. BAUSCHINGER [24], BAIRSTOW [25] and SANDOR [26]) observed, however, that the hysteresis which occurs when there are predominately tensile stresses differs considerably from that which occurs when the stresses are predominately compressive. In the former case, the micromechanisms of slip and microcracking contribute to fatigue behavior while in the latter case, slip alone may be the only significant micromechanism which is operative in the fatigue process.

While fatigue behavior in general may be investigated by means of hysteresis strain energy studies, it has been shown elsewhere [27] that hysteresis itself deserves study apart from its obvious implications with respect to fatigue. The goal of many investigations concerning the fatigue of metals is to produce a workable theory which will make an accurate prediction of fatigue behavior possible based upon data taken from tests of a relatively small number of samples. As a result of the analysis presented herein, it appears that such a goal can be attained, using hysteresis strain energy as the basic quantity measured, only if behavior in tension and behavior in compression can be properly differentiated and the resulting differences adequately treated.

Security and Economy

Metal fatigue is a catastrophic failure condition that has the potentiality to affect almost any bridge. This potentiality for disaster certainly justifies the many measures adopted by bridge engineers to minimize the dangerous effects of fatigue on their constructions. Yet, despite more than a century of research into the causes of fatigue in metals, much remains to be learned.

There are many questions regarding fatigue behavior that urgently require answers if engineers are to continue to provide improvements in the security and economy of bridge constructions. Some of the most urgent of these questions are: First, why do metals exhibit different fatigue characteristics when subjected on the one hand to purely compressive stresses and on the other hand to purely tensile stresses? Second, what is the relationship between hysteresis strain energy and fatigue strength? Third, and last, to what extent do fatigue effects cumulate in a metal structure subjected to a long history of cyclicallyvarying stresses? When satisfactory answers to these and other important questions are obtained, it will, of course, become possible to make more accurate predictions of the fatigue strength of bridge constructions than is now the case.

The mechanism of local plastic deformation or "slip" and the mechanism of microcracking or "fracture" are widely believed to be the microscopic phenomena which cause the wellknown macroscopic manifestations of fatigue to appear. It is shown in this paper, by means of an incremental collapse model, that the micro-mechanism of local plastic deformation alone is sufficient to account for practically all of the macroscopic manifestations of fatigue behavior in compression and that the fracture micro-mechanism is useful to explain the additional macroscopic aspects of fatigue which are associated with tensile stresses. Furthermore, it is shown that if properly treated, hysteresis strain energy is a useful macroscopic indicator of the fatigue process in metals. It is believed that the very careful categorization and elucidation of hysteresis strain energy described in this paper will lead to further progress in the quest for an adequate, and scientifically satisfactory basis for the prediction of fatigue strength of metal structures under service conditions.

Notation

E Modulus of Elasticity or Young's Modulus.
I Second static moment of cross-sectional area of flexural member.
L Length of Flexural member.
M_p Bending moment at which a plastic hinge will form in flexural member.
N_f Fatigue life or number of cycles to rupture in fatigue.
N_F Extended incremental collapse life or number of cycles to failure of the model.
W_a The alternating plasticity load.
W_c The plastic collapse load.
W_s The incremental collapse load or "shakedown" load.
$W_{\max}$ Maximum load intensity applied to the structure.
$W_{\min}$ Minimum load intensity applied to the structure.
$\overline{W}$ Mean load intensity applied to the structure.
R Range of loads applied to the structure (equal to absolute value of difference between $W_{\max}$ and $W_{\min}$).
S General notation for strength (i.e. stress level) in fatigue strength versus fatigue life graphs.
S_{EL} Endurance limit or Fatigue limit.
δ_h Horizontal displacement of end 2 of member 1-2 relative to end 1 during the application of a horizontal load to the frame at location 2.

δ_v Vertical displacement of member 2-4 at the point 3 relative to its end during the application of a vertical load to frame at location 3.

ΔU_i Irrecoverable energy or hysteresis energy imparted to the model during the ith cycle of load application and removal.

U Cumulative hysteresis energy imparted to the model at the end of the Nth cycle of load application and removal.

U_F Extended incremental collapse toughness or the sum of all hysteresis energy increments occurring during a sequence of cycles of stress application carried on until failure by incremental collapse occurs.

β Ratio of vertical load to horizontal load applied to the portal fram structure.

σ Stress.

σ_a Stress amplitude.

σ_m Mean stress = $1/2\ (\sigma_{max} + \sigma_{min})$.

σ_{max} Maximum stress level.

σ_{min} Minimum stress level.

σ_R Range of stress (equal to absolute value of difference between σ_{max} and σ_{min}).

Ω_f Fatigue toughness or the sum of all hysteresis strain energy increments occurring during a sequence of cycles of stress application carried on until fatigue rupture.

Acknowledgements

I am grateful to Professors Thomas Erber and Kuang-Han Chu of IIT for their many helpful suggestions and encouragement and to Mr. Surendra Singh for writing a computer program to carry out many of the extensive computations involved in this work.

The support of the National Science Foundation provided through Grant No. GH-34664 was of benefit during the final phase of the research.

References

1. TIMOSHENKO, S.P.: Strength of Materials. Vol. II, Third Edition, D. Van Nostrand Company, Inc., Princeton, N. J., 1956, pp. 413 and 514.
2. JAECKEL, H.R.: Simulation, Duplication and Synthesis of Fatigue Load Histories. Sound and Vibration, Vol. 4, March, 1970, pp. 18 to 29.
3. MARTIN, J.F., TOPPER, T.H., AND SINCLAIR, G.M.: Computer-Based Simulation of Cyclic Stress-Strain Behavior with Applications to Fatigue. Materials Research and Standards, Journal ASTM, Vol. 11, No. 2, February 1971.
4. WETZEL, R.M.: A Method of Fatigue Damage Analysis. Ford Motor Company Scientific Research Staff Technical Report, September, 1971, privately published.
5. NEAL, B.G.: The Plastic Methods of Structural Analysis. Chapman and Hall, London, 1956, Chapter V.
6. NEAL, B.G., and SYMONDS, P.S.: Cyclic Loading of Portal Frames, Theory and Tests. Publ. Intern. Assoc. of Bridge and Structural Engineer, Vol. 18, 1958, pp. 171–199.
7. GURALNICK, S.A.: Incremental Collapse Under Conditions of Partial Unloading. Publ. Intern. Assoc. of Bridge and Structural Engineers, Vol. 33, part II, September, 1973.
8. GERBER, W.: Bestimmung der zulässigen Spannungen in Eisenkonstructionen. Z. bayer. Architekten u. Ing. - Ver., 1874.

9. GOODMAN, J.: Mechanics Applied to Engineering. Longmans, Green and Company, London, 1899.
10. FÖPPL, O.: The Practical Importance of the Damping Capacity of Metals, Especially Steels. Journal of the Iron and Steel Institute, Vol. 134, 1936.
11. HALFORD, G.R.: The Energy Required for Fatigue. Journal of Materials. Vol. 1, No. 1, March 1966, pp. 3–18.
12. STÜSSI, Fritz: Die Dauerfestigkeit und die Versuche von August Wöhler. Mitt. der T.K.V.S.B., No. 13, Verlag V.S.B., Zurich, 1955.
13. HORNE, M.R.: Plastic Theory of Structures. MIT Press, Cambridge, Mass., 1971, p. 126.
14. PALMGREN, A.: Die Lebensdauer von Kugellagern. Zeitschrift des Vereins Deutscher Ingenieure, Vol. 68, 1924.
15. MINER, M.A.: Cumulative Damage in Fatigue. Journal of Applied Mechanics, Vol. 12, No. A-159, 1945.
16. GROVER, H.J.: An Observation Concerning the Cycle Ratio in Cumulative Damage. Symposium on Fatigue of Aircraft Structures. American Society for Testing and Materials, Special Technical Publication No. 274, 1960.
17. KAECHELE, L.: Review and Analysis of Cumulative Fatigue Damage Theories. The RAND Corp. Report RM-3650-PR, August 1963.
18. LEVE, H.L.: Cumulative Damage Theories. Chapter 6, Metal Fatigue, Edited by A.F. Madayag, John Wiley and Sons, Inc., New York, 1969.
19. FELTNER, C.E.: Strain Hysteresis, Energy and Fatigue Fracture. Report No. 146 of the Department of Theoretical and Applied Mechanics, University of Illinois, Urbana, Ill., June, 1959.
20. MARTIN, D.E.: An Energy Criterion for Low-Cycle Fatigue. Trans. ASME, Journal of Basic Engineering, December 1961, pp. 565–570.
21. MORROW, J.D.: Cyclic Plastic Strain Energy. To be found in Special Technical Publication, No. 378, entitled, "Internal Friction, Damping, and Cyclic Plasticity", published by the American Soc. for Testing and Materials, Philadelphia, Pa., 1965.
22. CHANG, C.S., PIMBLEY, W.T. and CONWAY, H.D.: An Analysis of Metal Fatigue Based on Hysteresis Energy. Experimental Mechanics, Journal of the SESA, March 1968, pp. 133–137.
23. LANDGRAF, R.W., MORROW, J.D., and ENDO, T.: Determination of the Cyclic Stress-Strain Curve. Journal of Materials, Vol. 4, No. 1, March 1969, pp. 176–188.
24. BAUSCHINGER, J.: Über die Veränderungen der Elastizitätsgrenze und der Festigkeit des Eisens und Stahls durch Strecken, Quetschen, Erwärmen, Abkühlen und durch oftmals wiederholte Belastung. Mitt. Tech. Lab., Munich, Vol. 13, 1886.
25. BAIRSTOW, L.: The Elastic Limits of Iron and Steel Under Cyclical Variations of Stress. Philosophical Transactions of the Royal Society, London, Series A, Vol. 210, p. 35, 1911.
26. SANDOR, B.I.: Fundamentals of Cyclic Stress and Strain. University of Wisconsin Press, Madison, 1972.
27. ERBER, T., GURALNICK, S.A., and LATAL, H.G.: A General Phenomenology of Hysteresis. Annals of Physics, Published by Academic Press, Inc., Vol. 69, No. 1, January 1972, pp. 161–192.

Summary

Many of the phenomena observed in connection with fatigue of metal structures subjected to long-term, cyclically-varying loads remain unexplained. The stress-strain hysteresis exhibited by a metal structure or specimen when it is subjected to cyclically-varying loads has long been considered to be an important indicator of fatigue characteristics. Unfortunately, a means of satisfactorily linking stress-strain hysteresis with fatigue strength has hitherto been lacking. It is shown by means of an incremental collapse model that a process of localized plastic deformation (or "slip") is sufficient to cause fatigue rupture even under conditions where only purely compressive stresses exist. Hence, the differences in fatigue behaviour of the same material when subjected on the one hand to purely compressive stresses and the other hand to purely tensile stresses is explained.

Résumé

De nombreux phénomènes relatifs à la fatigue sous charges cycliques, variables et de longue durée, restent encore inexpliqués. L'hystérèse contrainte/allongement de structures ou d'éléments en métal sous une charge cyclique variable a été longtemps considérée comme une caractéristique importante de la fatigue. Mais il manquait une relation entre cette hystérèse et la résistance à la fatigue. Un modèle incrémental de rupture a permis de démontrer qu'un processus de déformation plastique limitée suffit à provoquer une rupture de fatigue, même en la seule présence de contraintes de compression. Les différences dans le comportement à la fatigue d'un même matériau sont ainsi expliquées, selon qu'il s'agit exclusivement de contraintes de compression ou de traction.

Zusammenfassung

Zahlreiche Phänomene der Metallermüdung unter lange wirkenden zyklisch variierenden Lasten bleiben ungeklärt. Die Spannungs/Dehnungs-Hysterese, die an Metallbauten oder -proben auftritt, wenn diese zyklisch variabler Belastung ausgesetzt sind, wurde lange als wichtiges Merkmal des Ermüdungsverhaltens betrachtet. Leider fehlte bisher eine befriedigende Beziehung zwischen der Spannungs-Dehnungs-Hysteresis und der Ermüdungsfestigkeit. An einem inkrementalen Modell wird gezeigt, dass ein Prozess örtlich begrenzter plastischer Verformungen (bzw. „Schiebungen") genügt, um Ermüdungsbrüche sogar unter Anwesenheit reiner Druckbeanspruchung herbeizuführen. Deshalb werden die Unterschiede im Ermüdungsverhalten desselben Materials erklärt, wenn dieses einerseits reiner Druckbeanspruchung, anderseits reiner Zugbeanspruchung ausgesetzt ist.

Leere Seite
Blank page
Page vide